Supplement of Geosci. Model Dev., 18, 6313–6340, 2025
https://doi.org/10.5194/gmd-18-6313-2025-supplement

Geoscientific Model Development
Open Access
EGU

Supplement of

Constraining CMIP6 sea ice simulations with ICESat-2

Alek Petty et al.

Correspondence to: Alek Petty (akpetty@umd.edu)

Supplement

Includes:

Fig S1: Arctic Ocean mean area results for recent period compared to SIMIP.

Figs S2-S3: Evaluation of regridding impacts.

Figs S4: Evaluation of interpolation/smoothing procedure on ATL20

Figs S5: Bulk ice density assessment including ACCESS-CM2

Figs S6-S18: Plausibility plots for all different hemispheres and metrics not included in the main manuscript.

Fig S19: Constrained seasonal analysis of area, total freeboard and thickness.

Figs S20-S31: Spatial bias plots for all different hemispheres and metrics not included in the main manuscript.

Figs S32-S35: Composite maps for the two different time periods not included in the main manuscript.

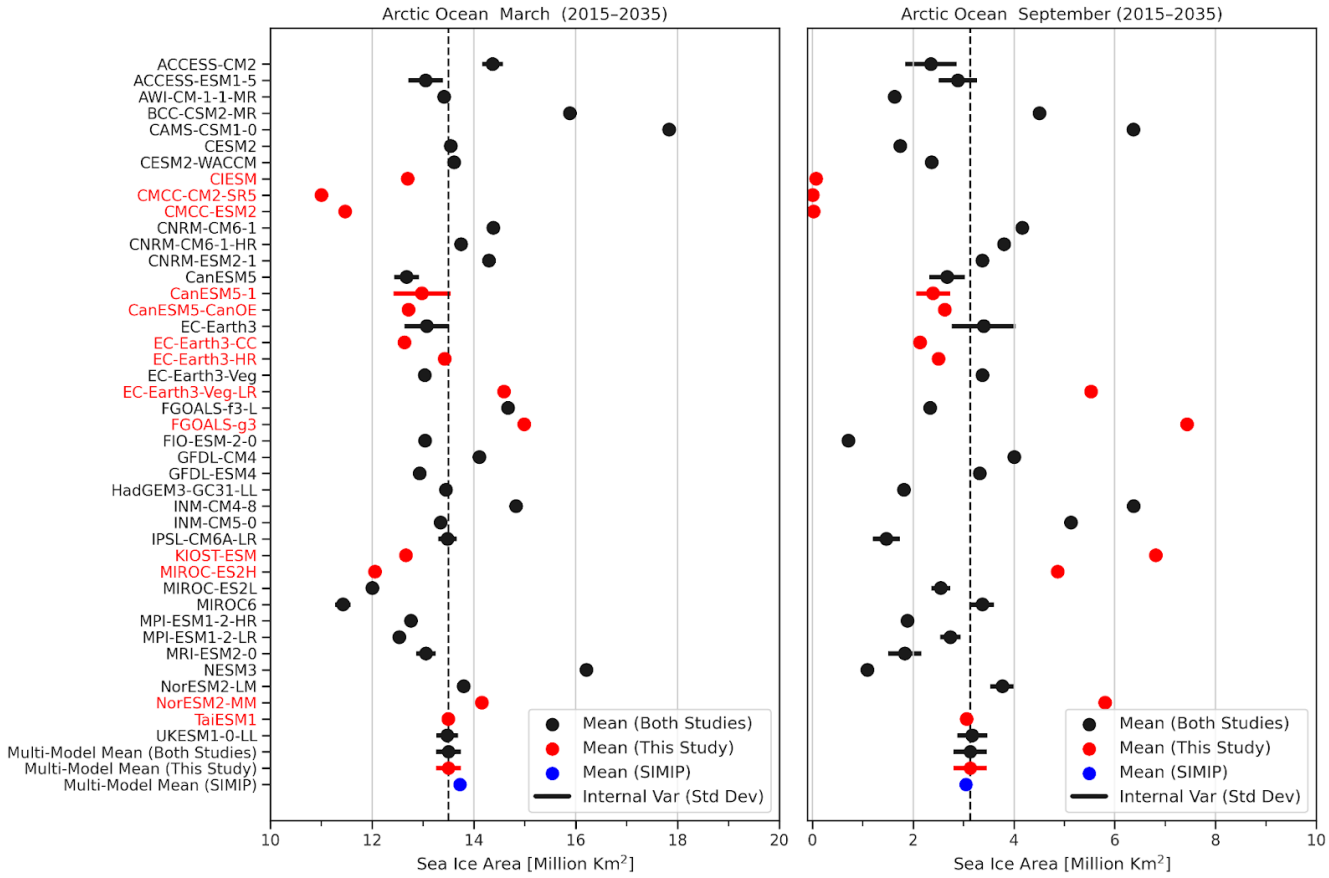

Figure S1: CMIP6 simulations of mean Arctic sea ice area over a 2015 to 2025 period in March (left) and September (right), comparing results across models used in SIMIP2020, our study, and both. Horizontal lines show the internal variability (1 standard deviation of the available ensemble spread).

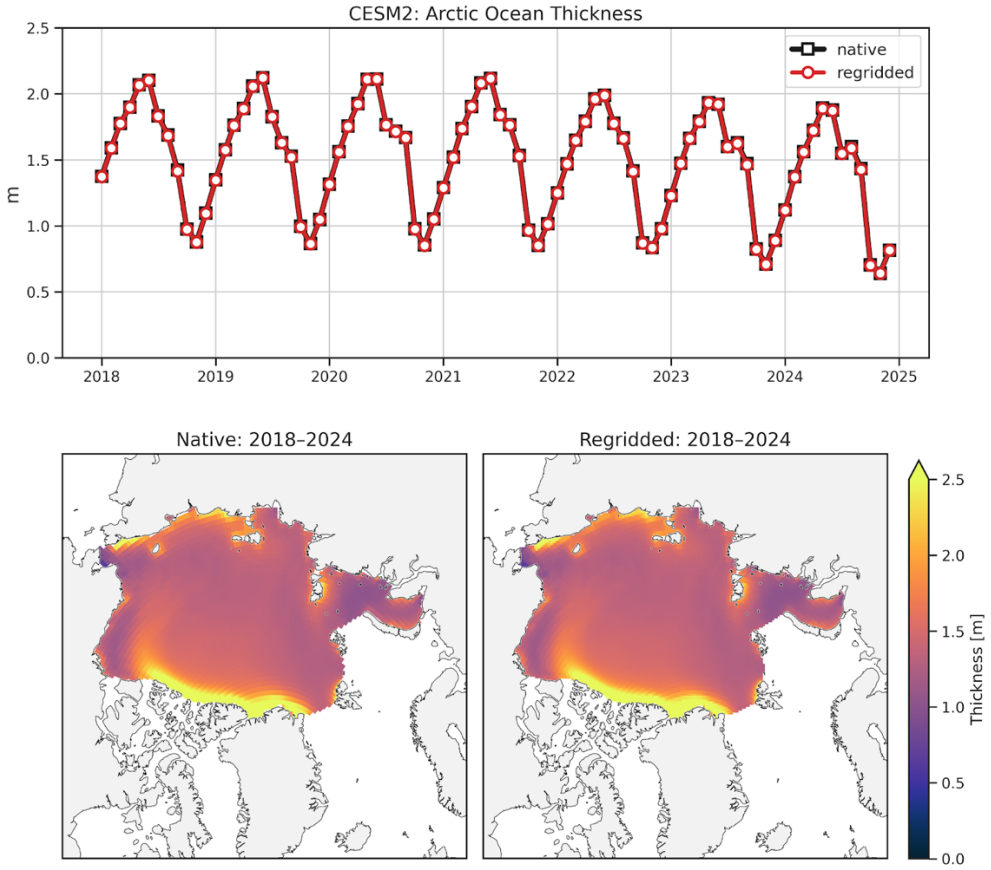

Figure S2: Impact of model regridding of CESM thickness output from the native grid to the 25 km x 25 km polar stereographic grid. Regridding using the conservative normed algorithm in xESMF.

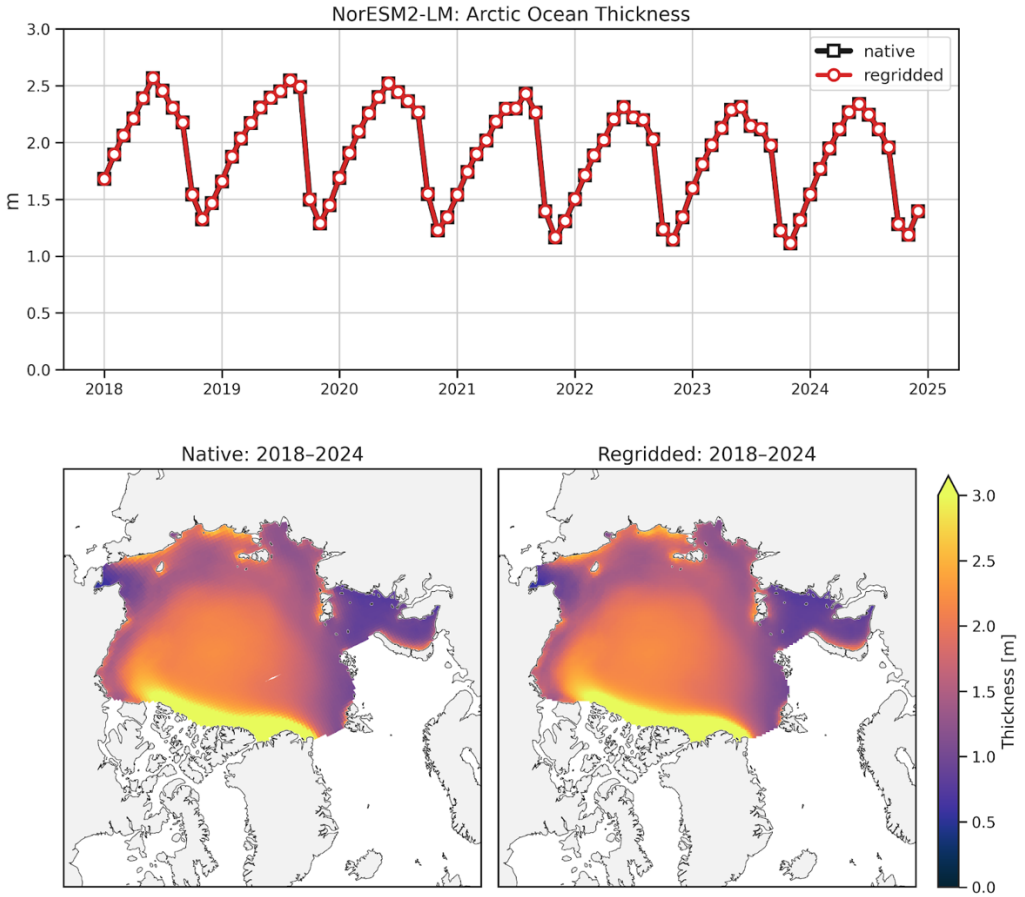

Figure S3: As in Fig. S2 but for the NorESM2-LM model.

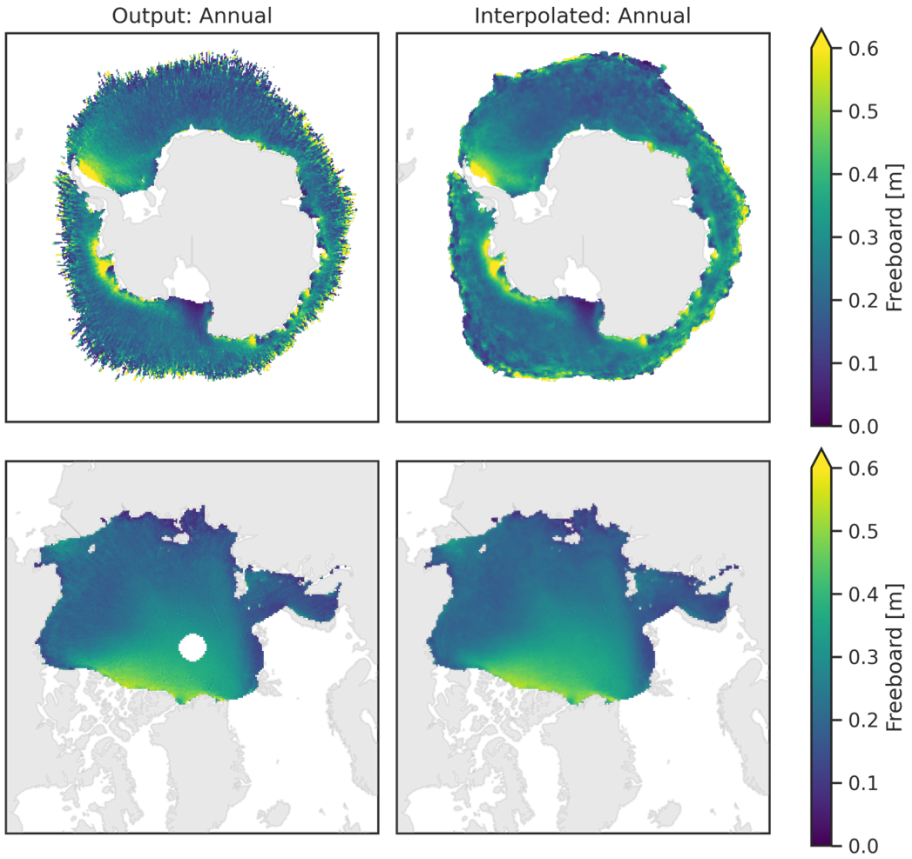

Figure S4: Annual mean (2018 to 2024) total freeboard from ATL20 v4 over the Southern Ocean (top) and Arctic Ocean (bottom) using just the raw data (left) and then using the smoothed/Gaussian interpolated data, as

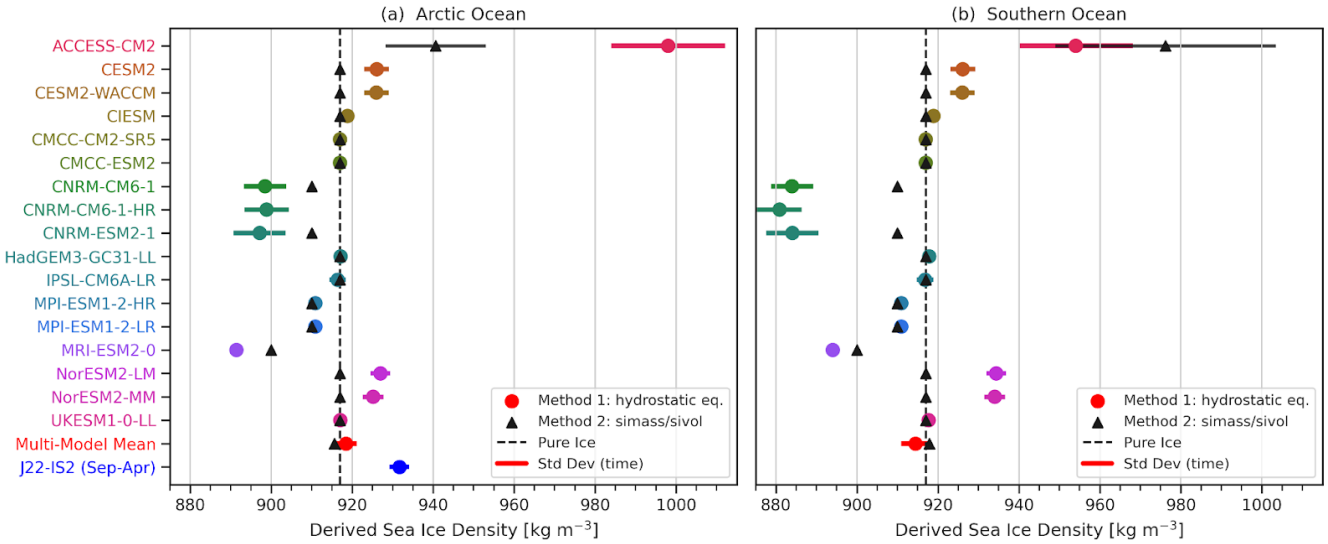

Figure S5: As in Fig. 4 of the main manuscript but including the ACCESS-CM2 model.

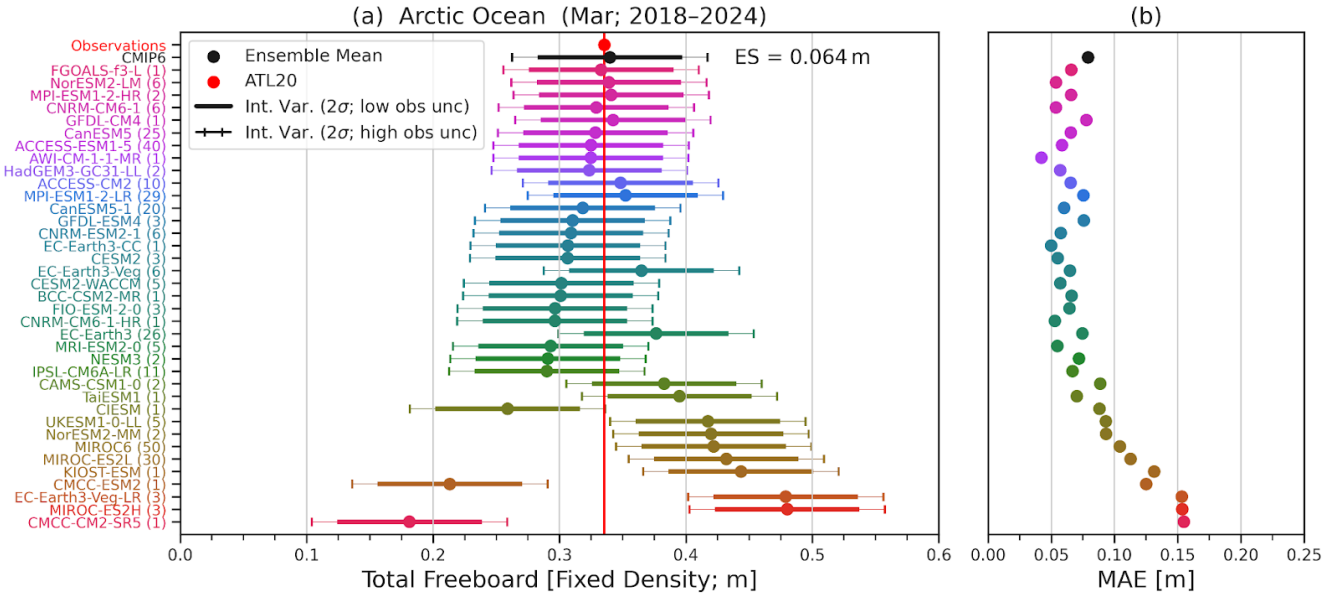

Figure S6: (a) As in Fig. 7 of the main manuscript but showing comparisons of March mean (2018 to 2024) Arctic Ocean total freeboard estimates from the 36-model CMIP6 subset (ensemble means, using a fixed ice density) and observations from ICESat-2 ATL20. Horizontal lines on each model show the plausibility window based on internal variability and both the low (bars) and high (whiskers) observational uncertainty estimates. The red circle and vertical red line shows the ATL20 observational mean. ES: ensemble spread. (b) Mean Absolute Error (MAE) of the spatial differences across the 25 km x 25 km grid-cells.

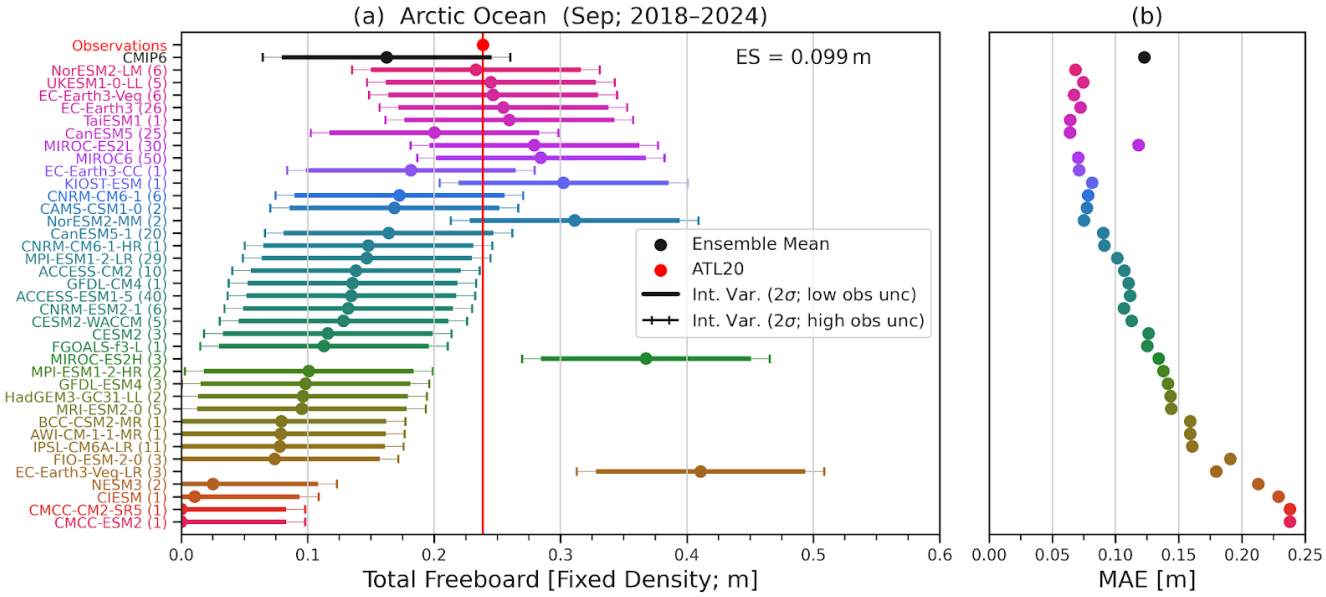

60 **Figure S7:** As in Fig. S4 but for September.

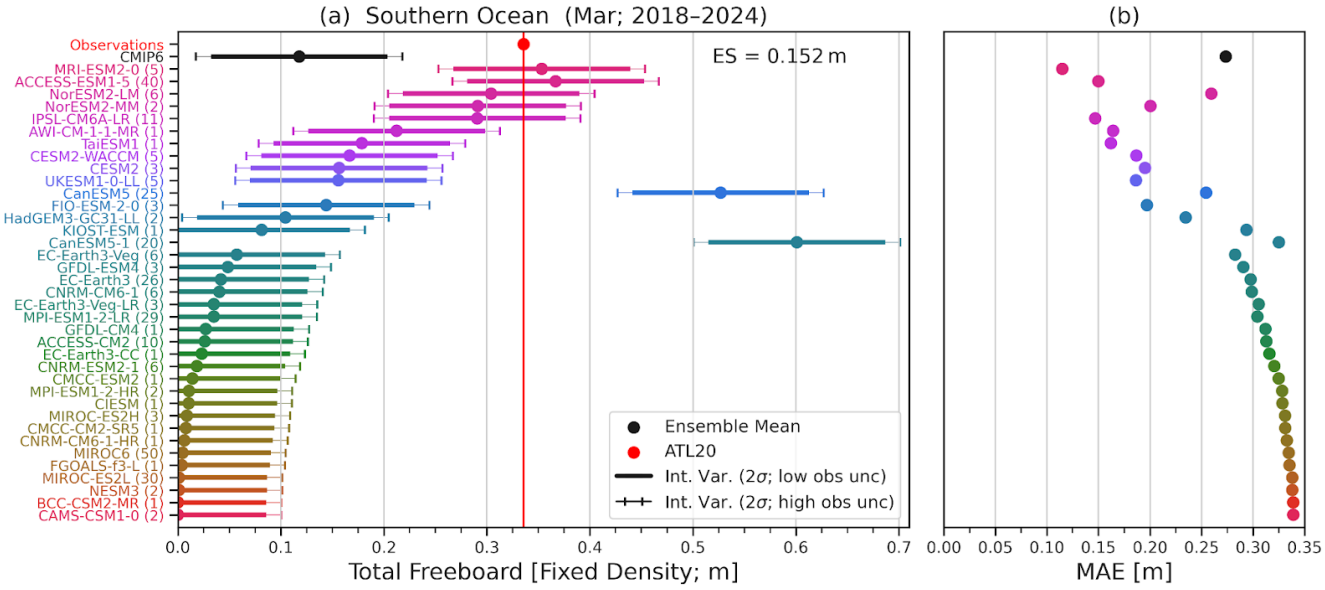

Figure S8: As in Fig. S4 but for March over the Southern Ocean.

65

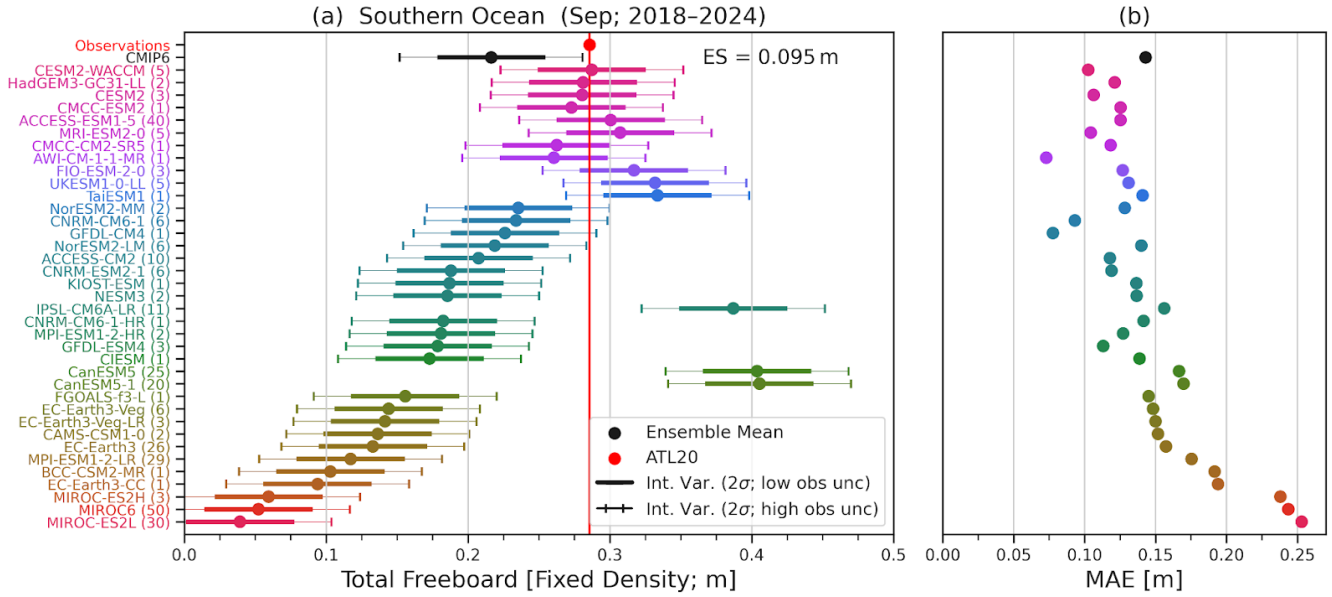

Figure S9: As in Fig. S4 but for September over the Southern Ocean.

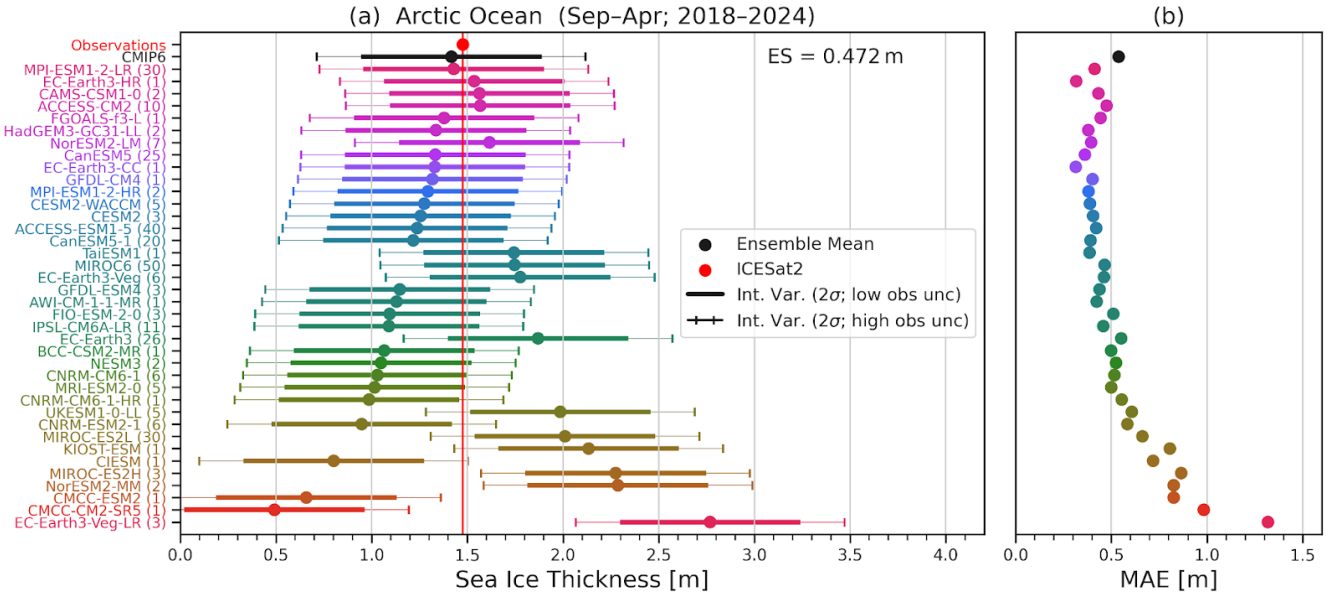

Figure S10: As in Fig. S4 but for Annual (September to April due to data availability) sea ice thickness over the Arctic Ocean.

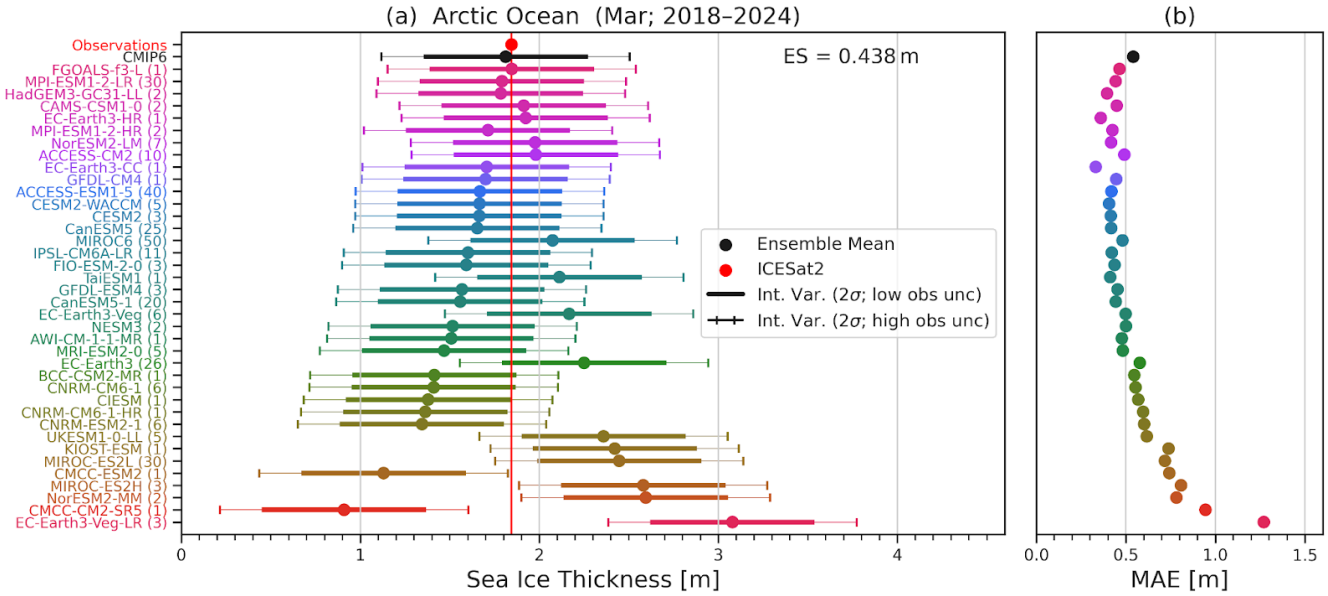

75 **Figure S11:** As in Fig. S4 but for March sea ice thickness over the Arctic Ocean.

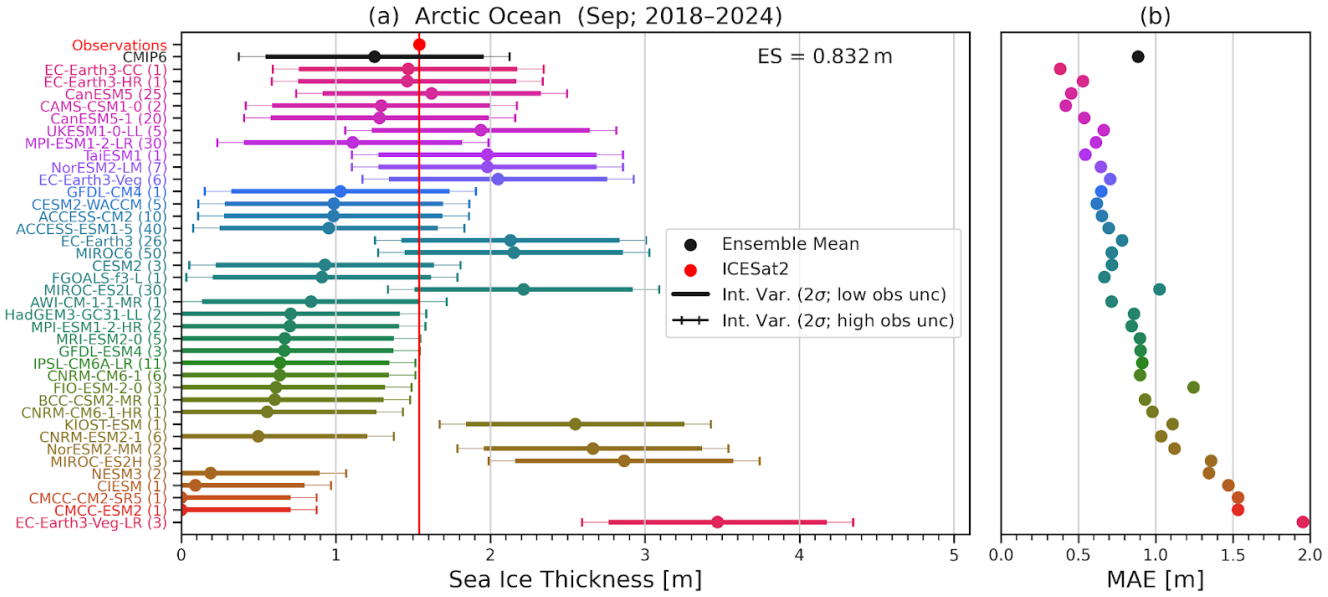

Figure S12: As in Fig. S4 but for September sea ice thickness over the Arctic Ocean.

80

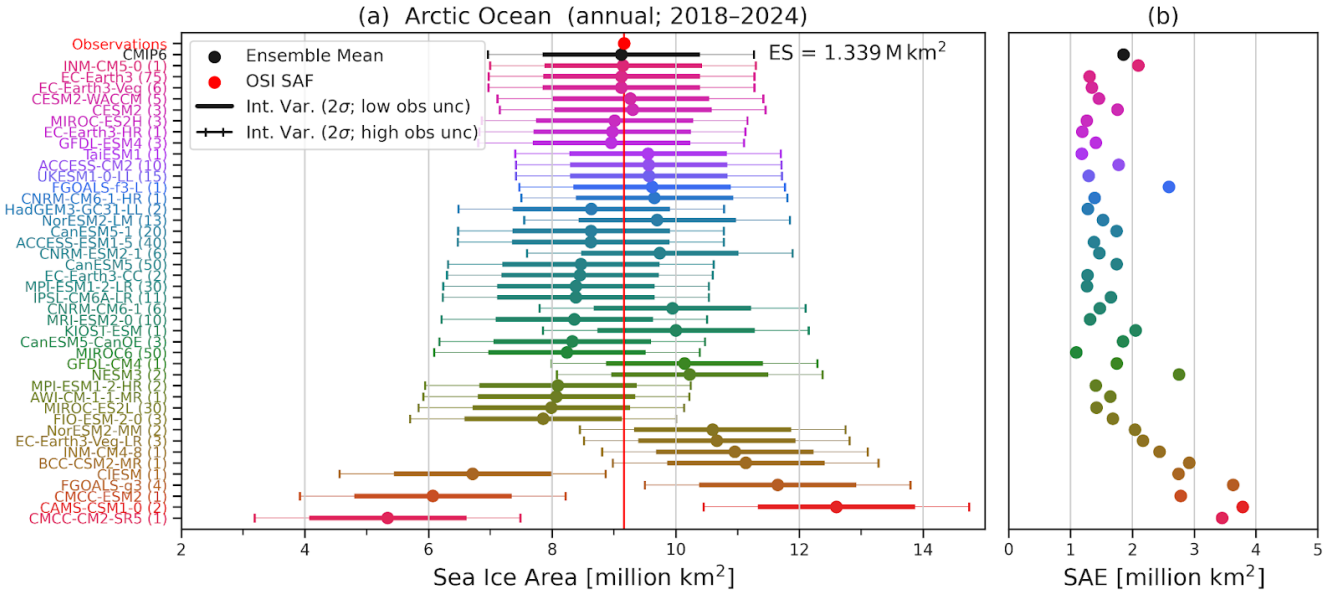

Figure S13: As in Fig. S4 but for Annual mean sea ice area over the Arctic Ocean.

85

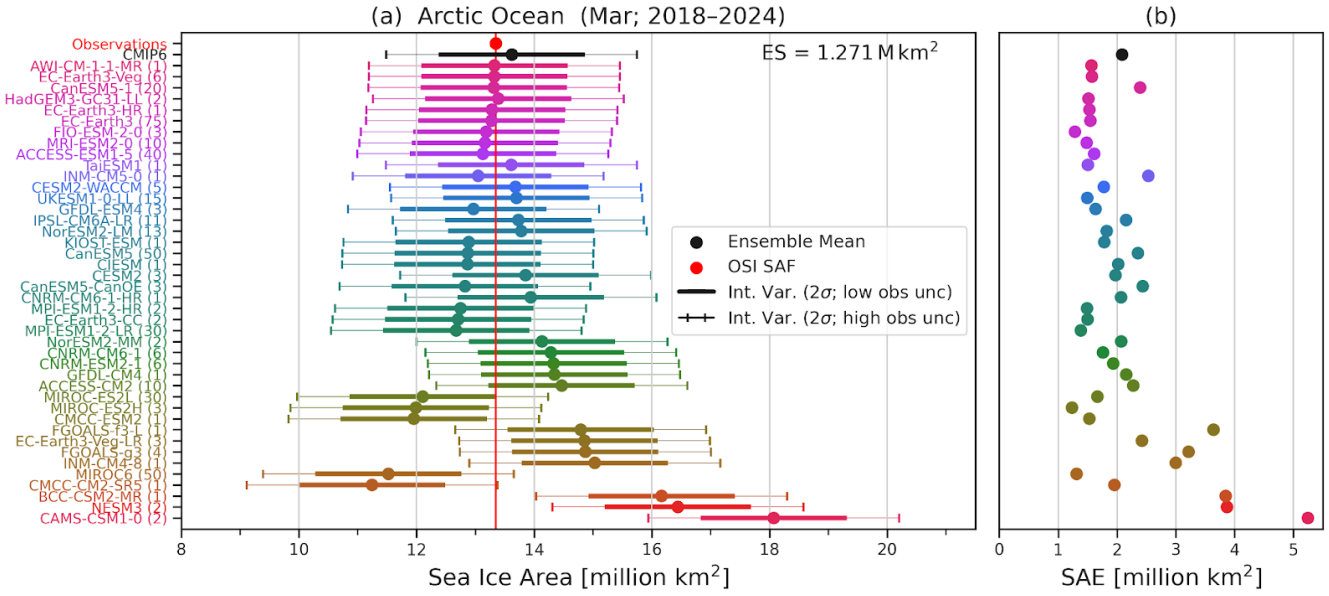

Figure S14: As in Fig. S4 but for March sea ice area over the Arctic Ocean.

90

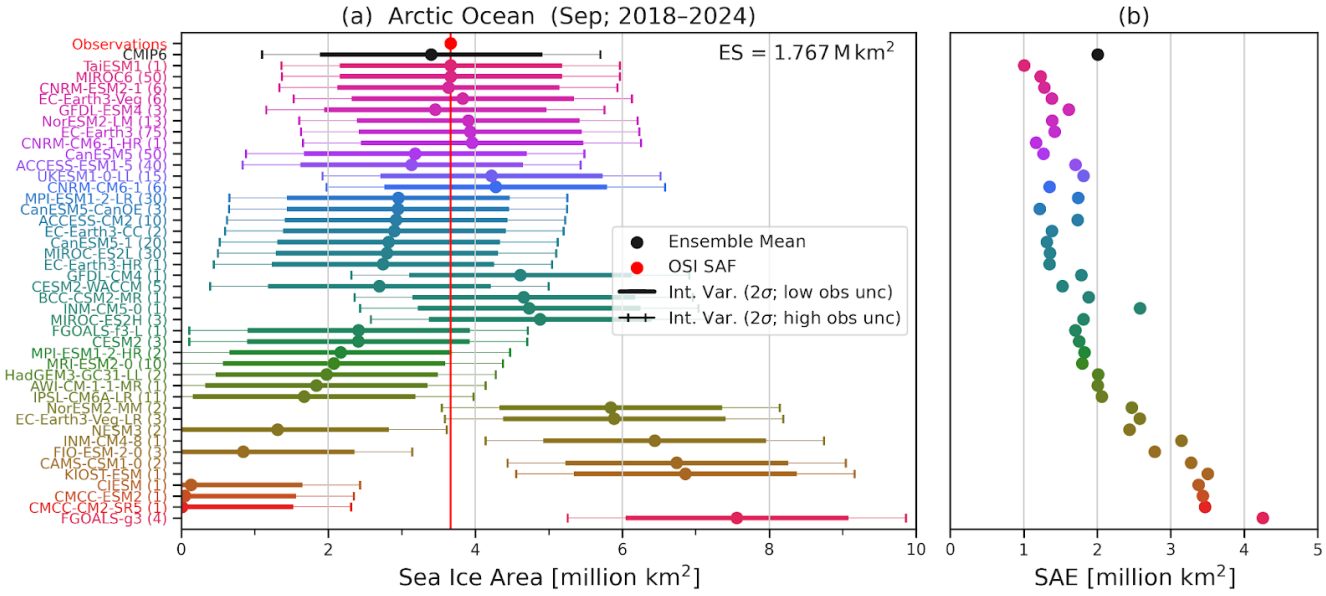

Figure S15 As in Fig. S4 but for September sea ice area over the Arctic Ocean.

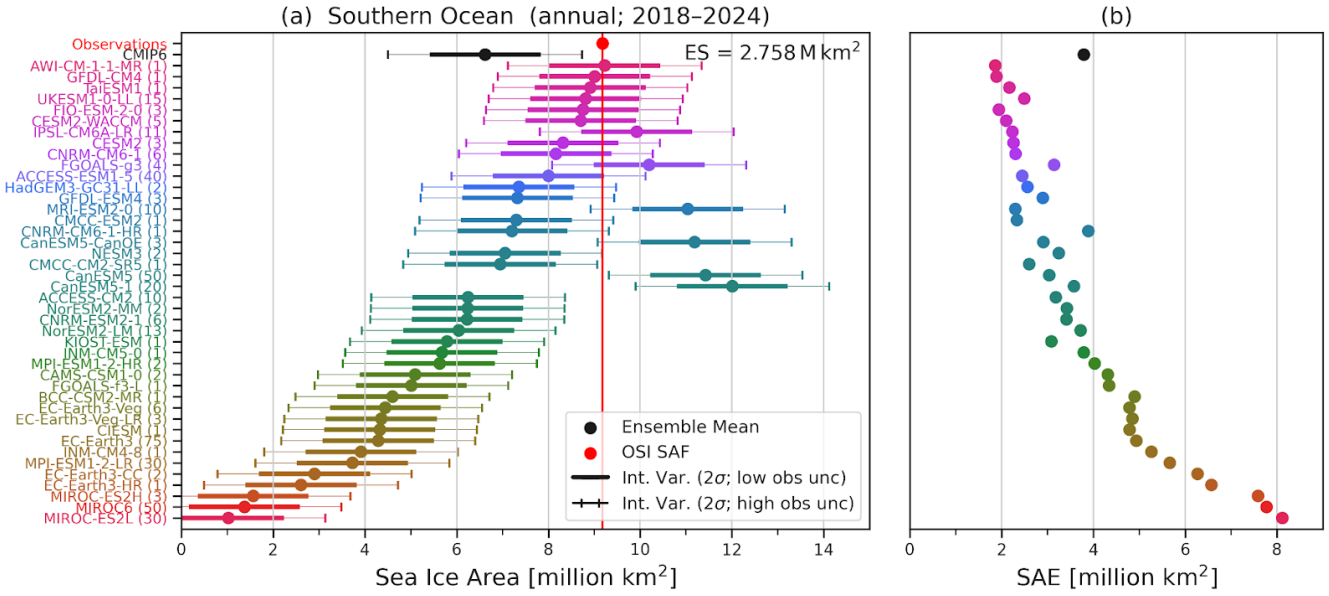

Figure S16: As in Fig. S4 but for Annual mean sea ice area over the Arctic Ocean.

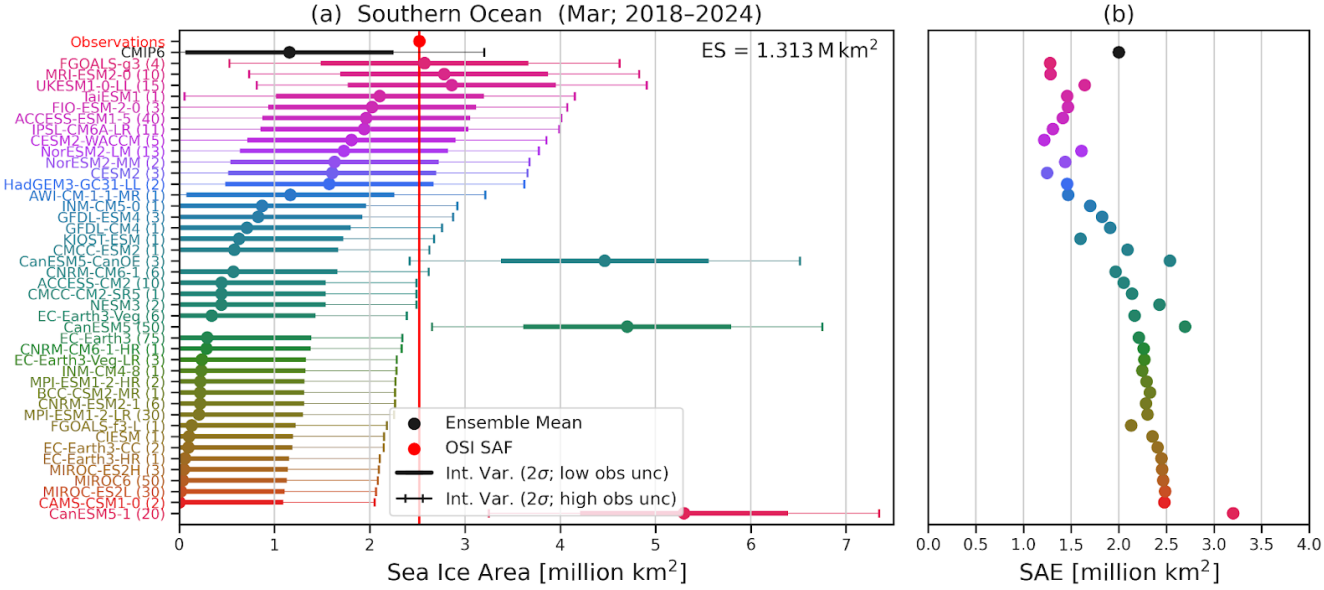

Figure S17: As in Fig. S4 but for March mean sea ice area over the Southern Ocean.

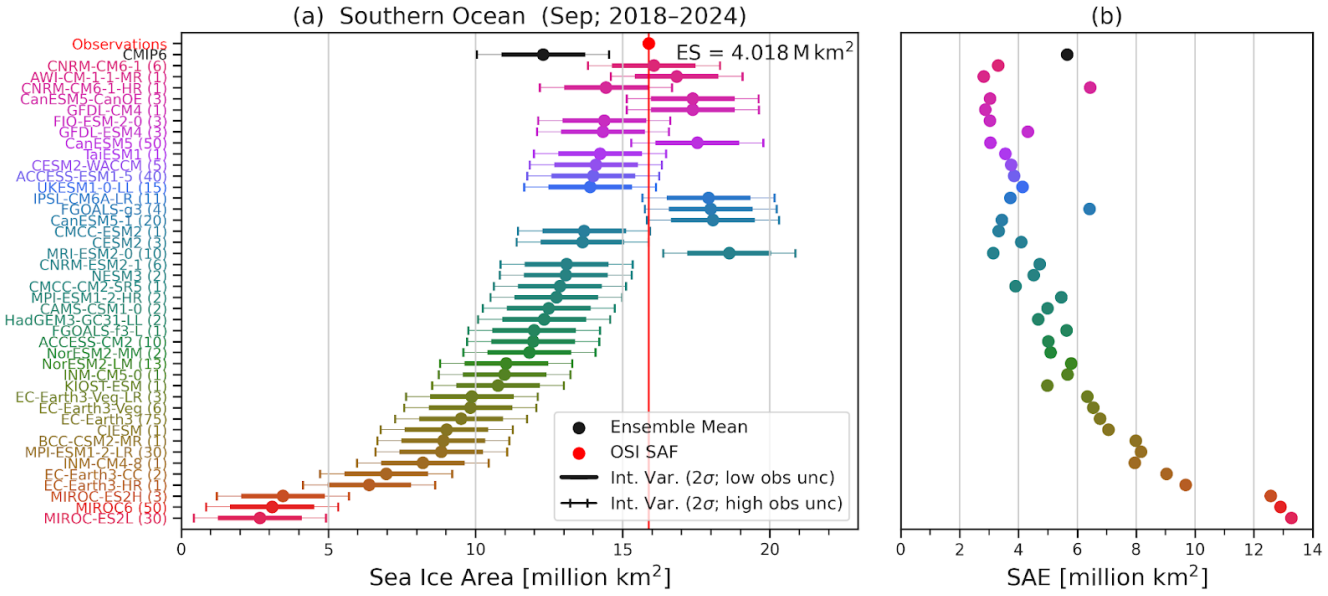

105 **Figure S18:** As in Fig. S4 but for September mean sea ice area over the Southern Ocean.

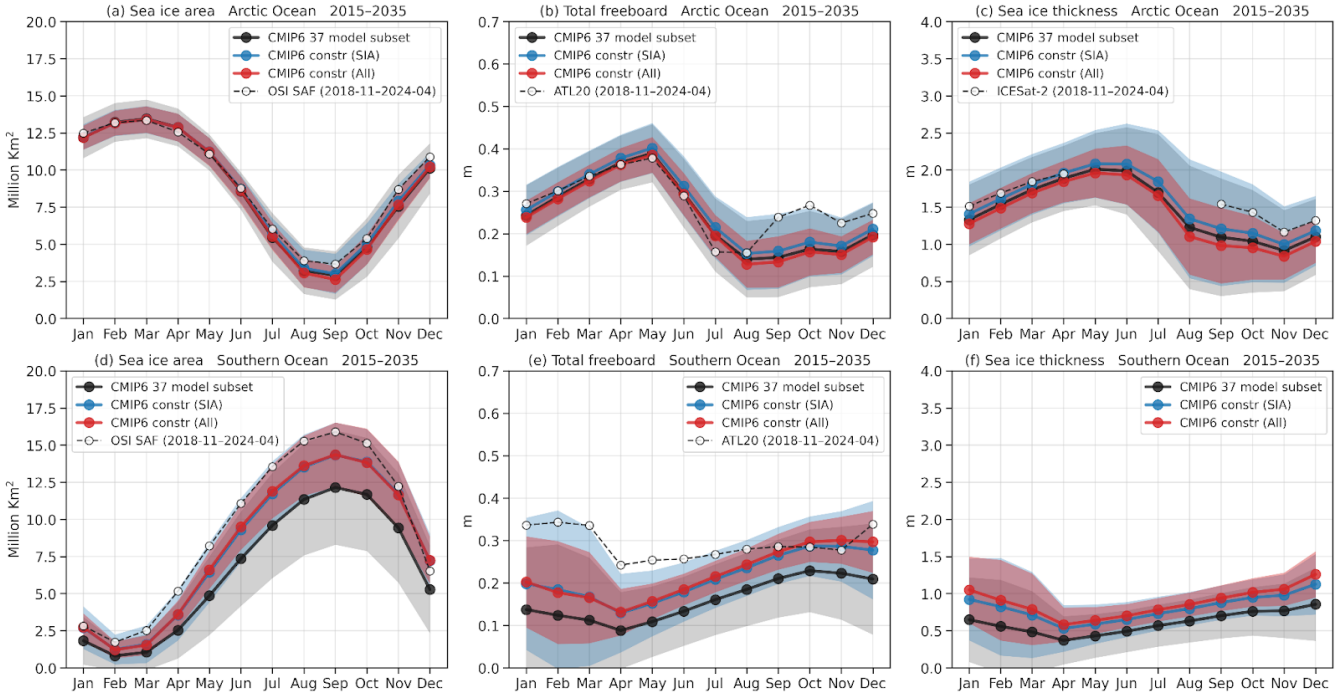

Figure S19: Seasonal CMIP6 ensemble mean (lines and circles) and ensemble spread (shading, one standard deviation) sea ice area (left), total freeboard (middle) and sea ice thickness (right) from the unconstrained 36-model subset (black), the annual area constrained subset (blue), and the subset constrained with all considered annual variables, including area and freeboard for both hemispheres, and the addition of sea ice thickness for the Arctic only (red). White circles/dashed lines show the observations, sea ice area from the OSI SAF passive microwave dataset, total freeboard from the ICESat-2 ATL20 (version 4), winter (September to April) Arctic sea ice thickness from the IS2SITMOGR4 (v3) dataset.

Figure S20: As in Fig. 11 of the main manuscript but for March.

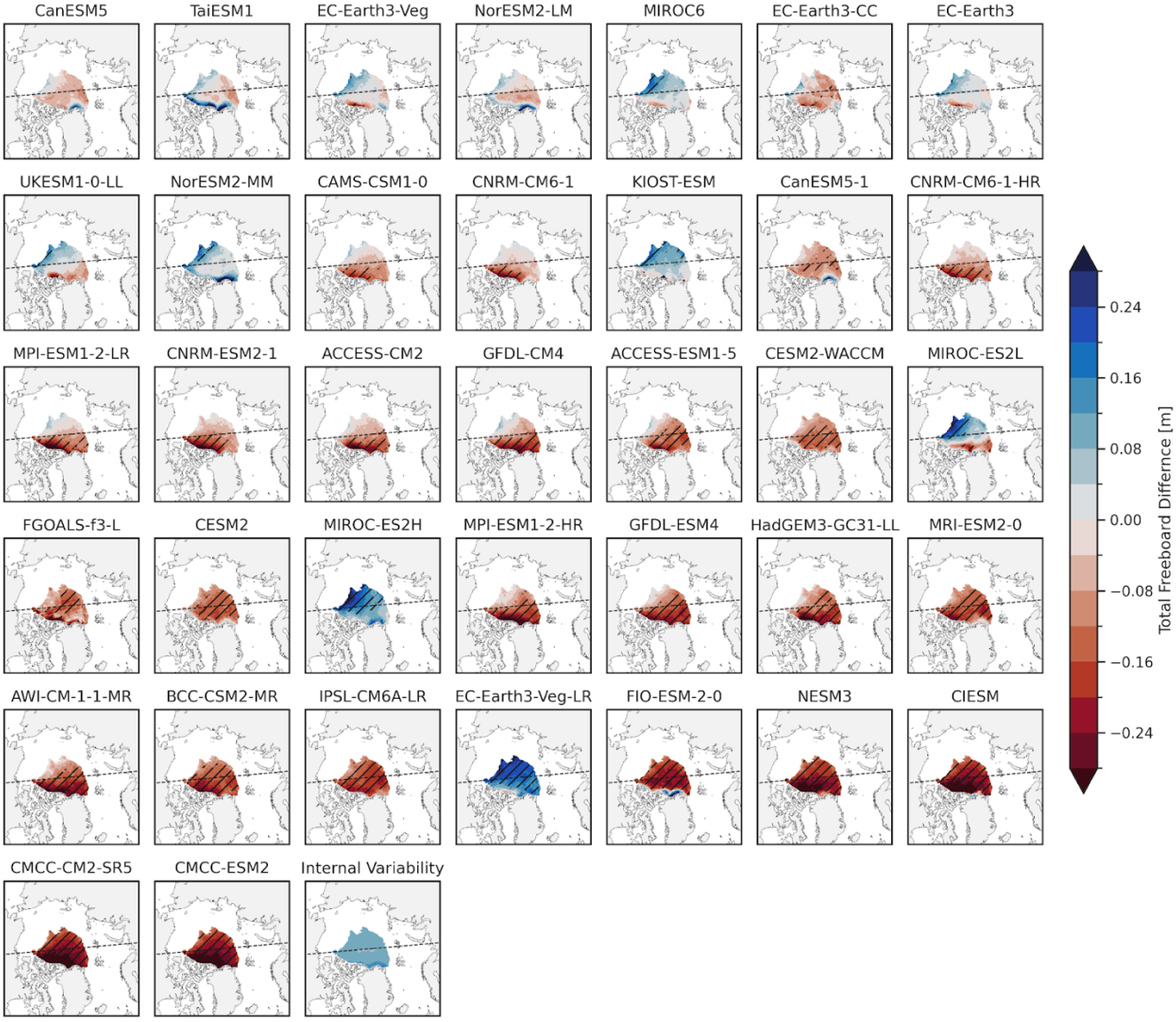

Figure S21: As in Fig. 11 of the main manuscript but for September.

125

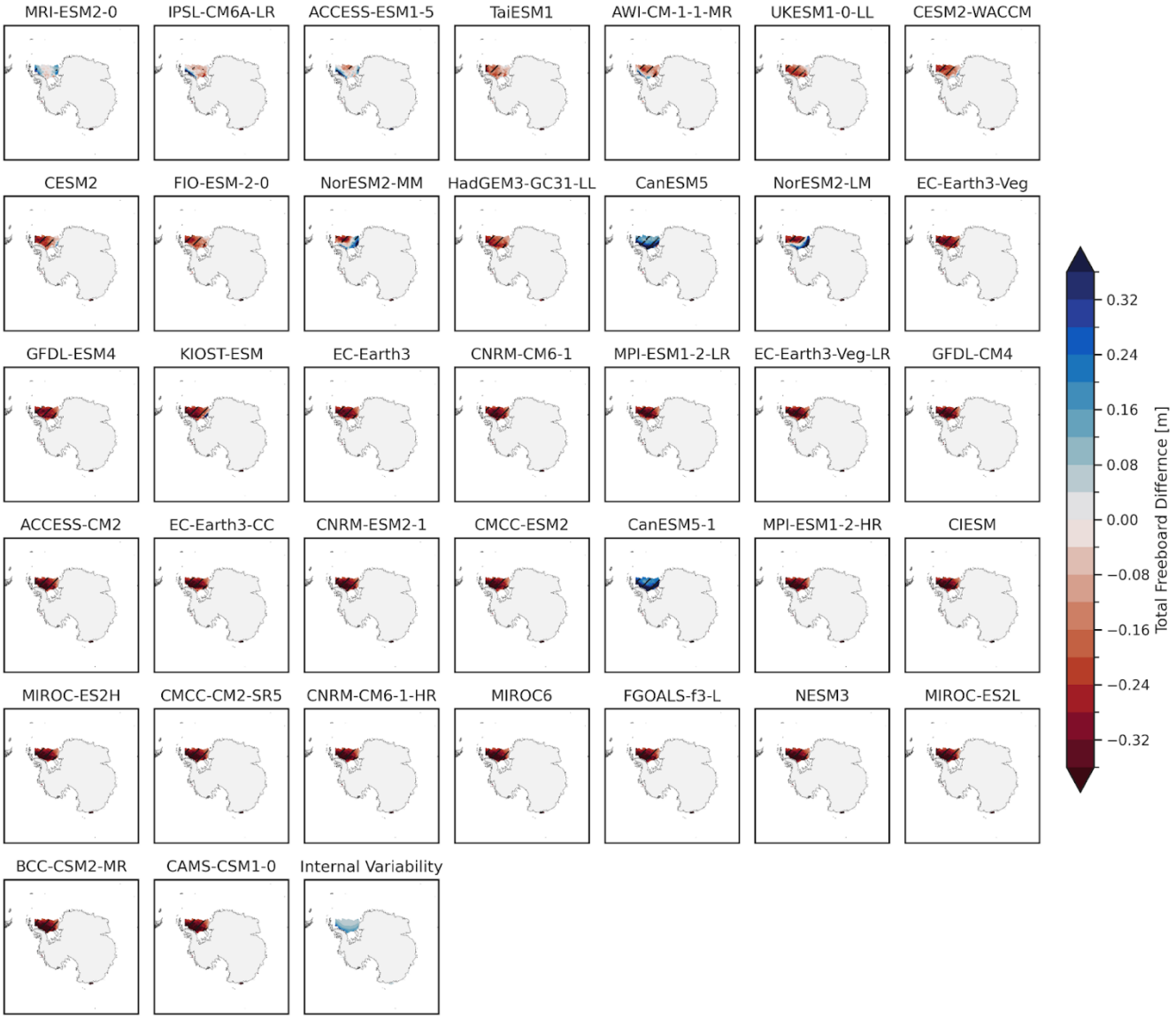

Figure S22: As in Fig. 13 of the main manuscript but for March over the Southern Ocean.

130

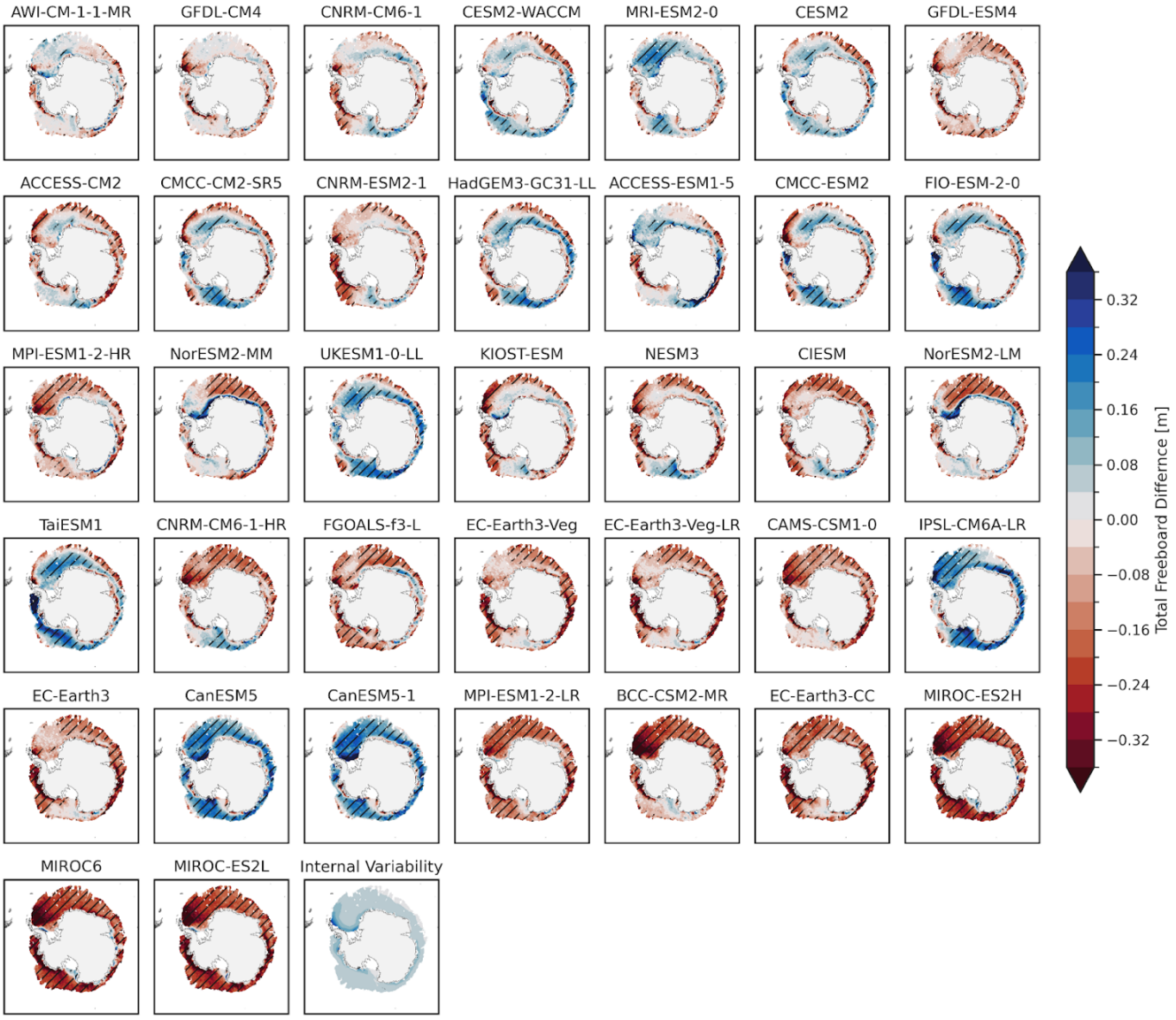

Figure S23: As in Fig. 13 of the main manuscript but for September over the Southern Ocean.

135

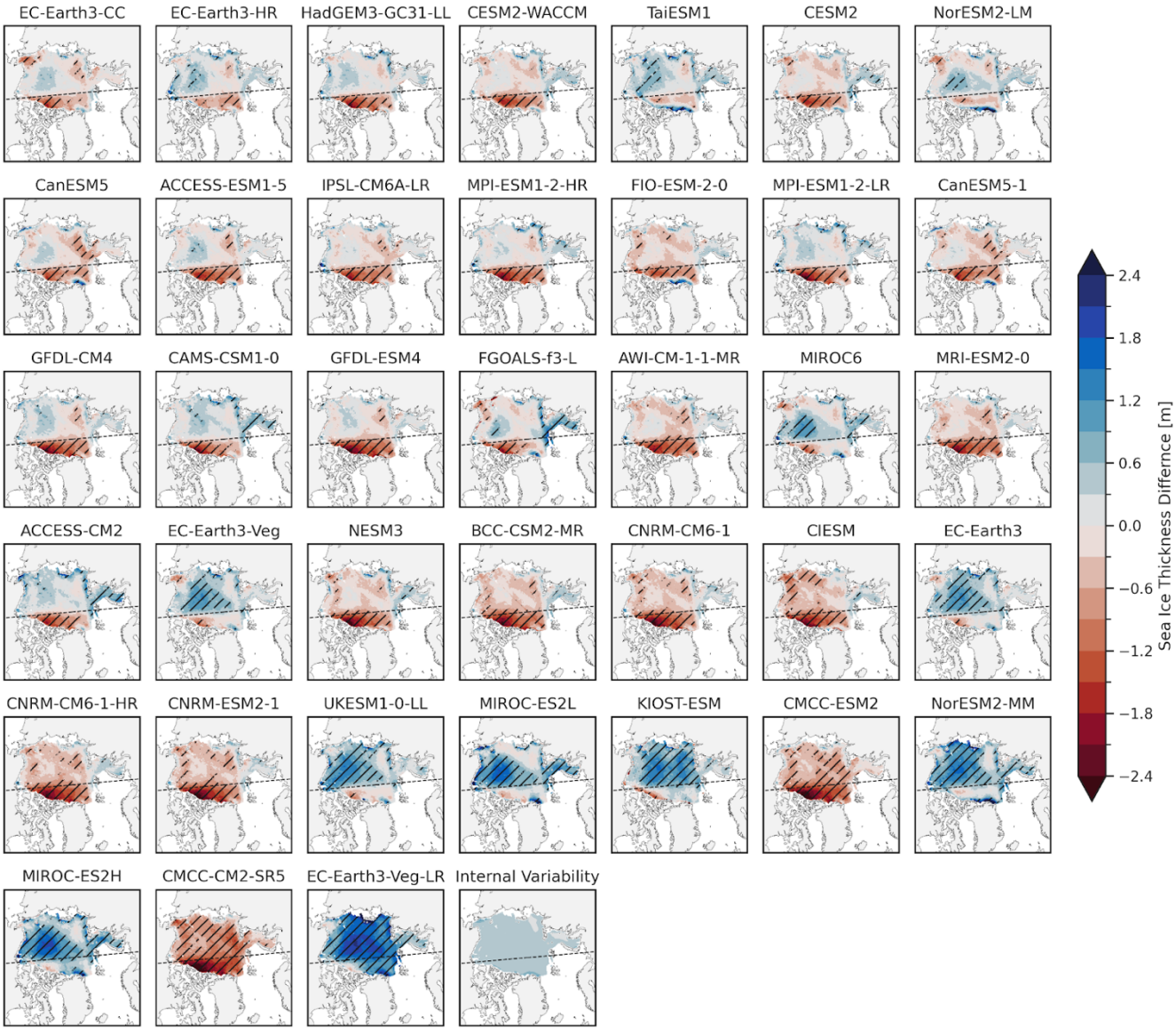

Figure S24: As in Fig. 11 of the main manuscript but for March sea ice thickness.

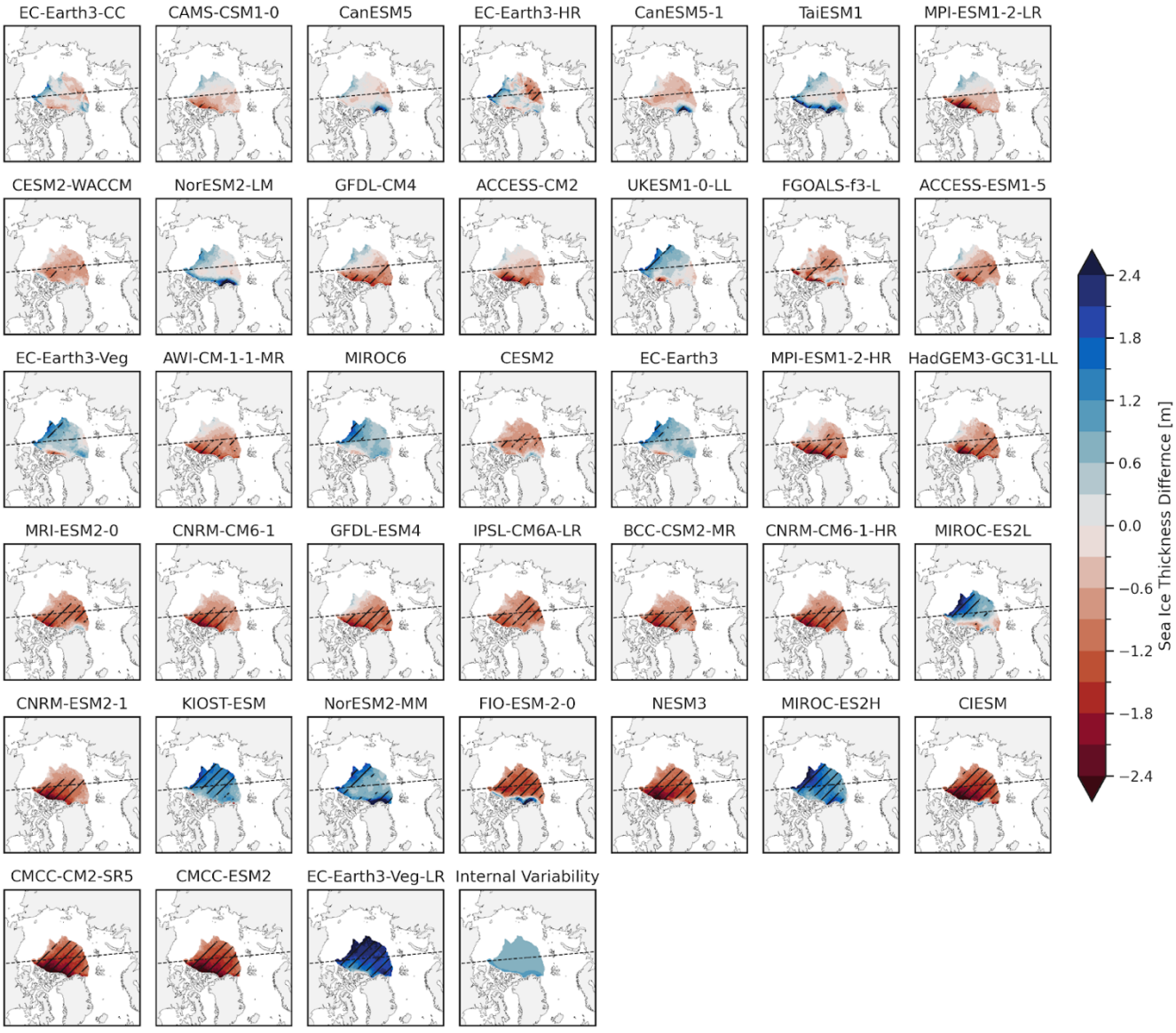

Figure S25: As in Fig. 11 of the main manuscript but for September sea ice thickness.

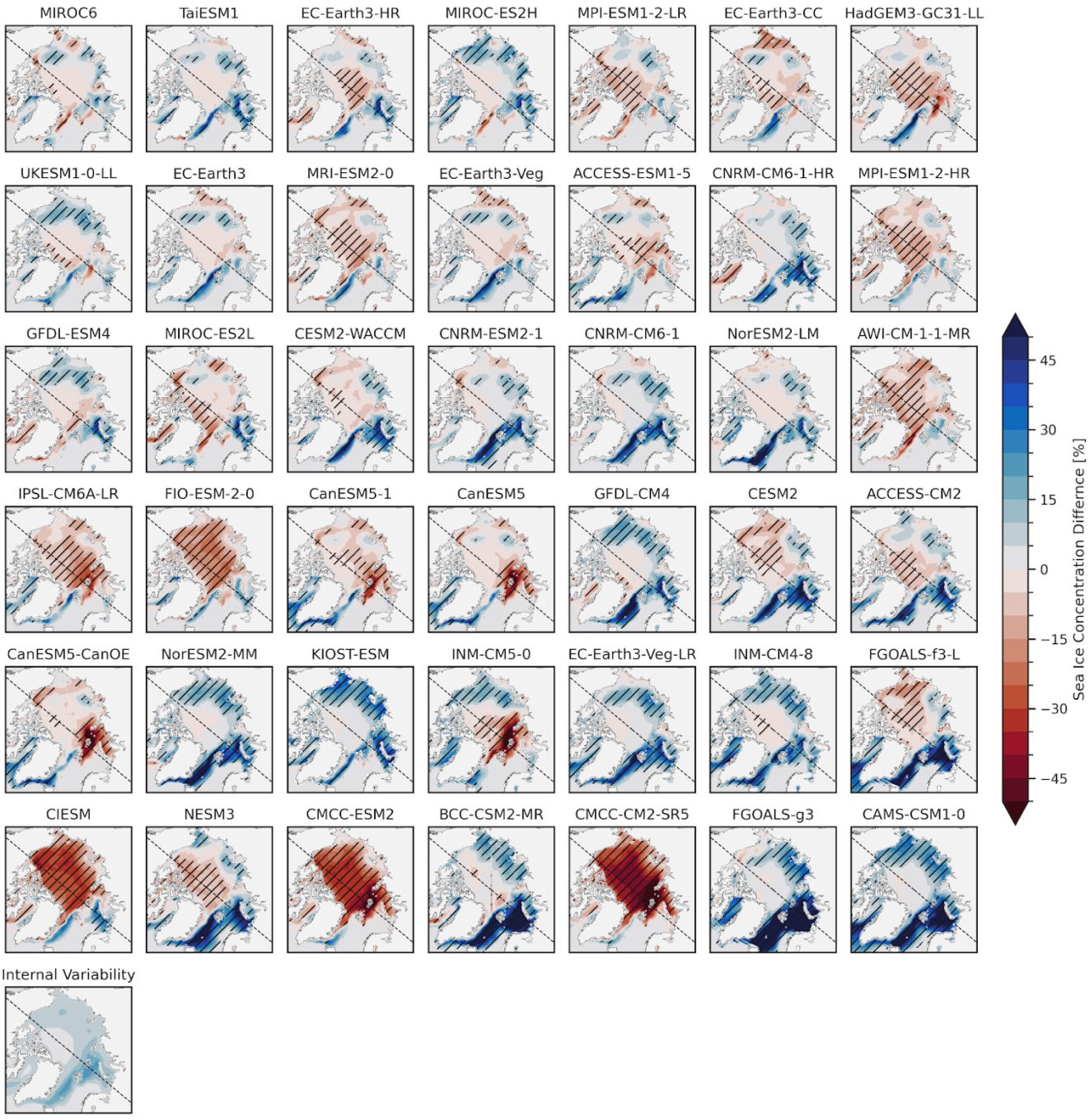

150 **Figure S26:** As in Fig. 11 of the main manuscript but for Annual sea ice concentration.

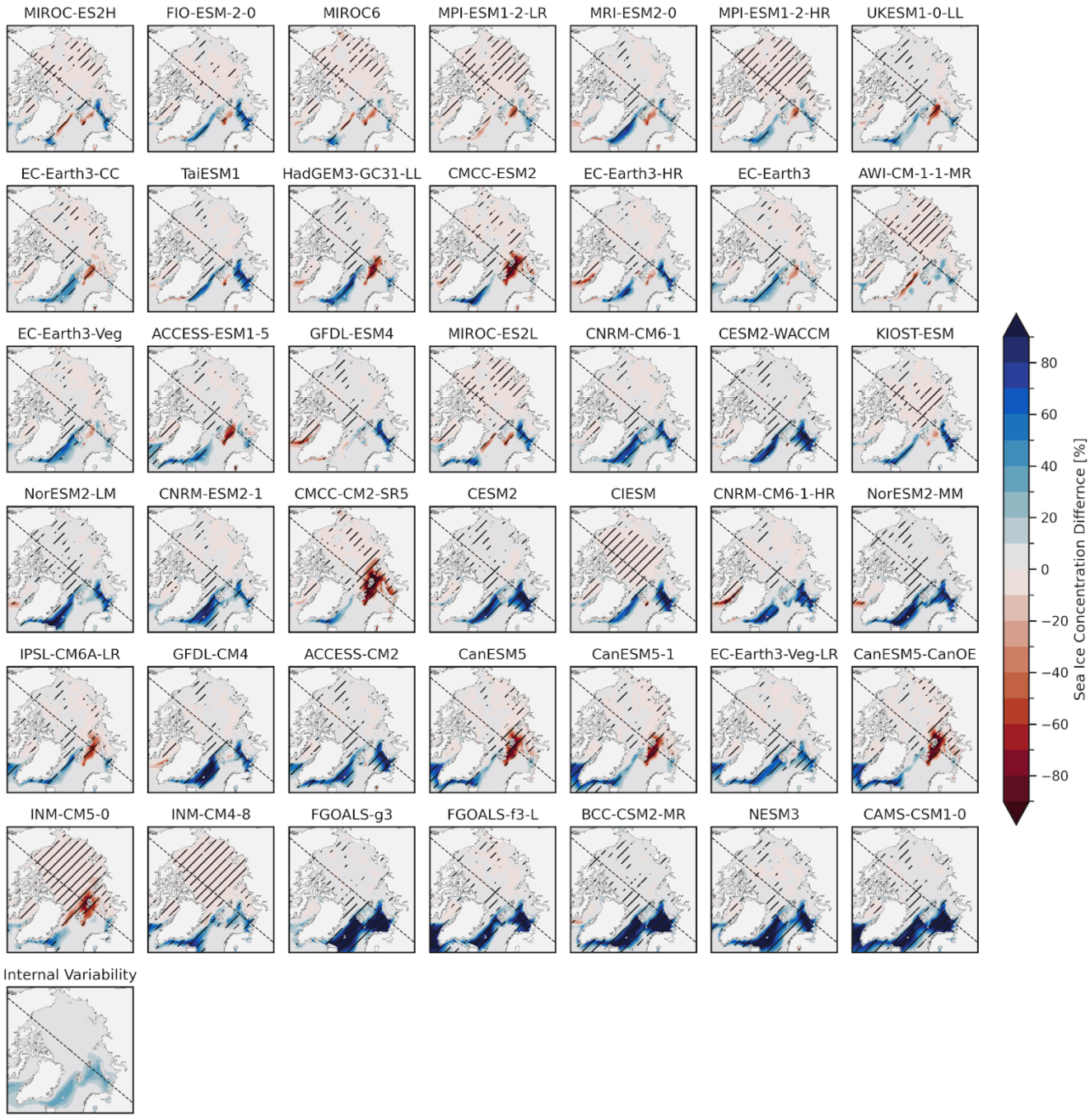

155 **Figure S27:** As in Fig. 11 of the main manuscript but for March sea ice concentration.

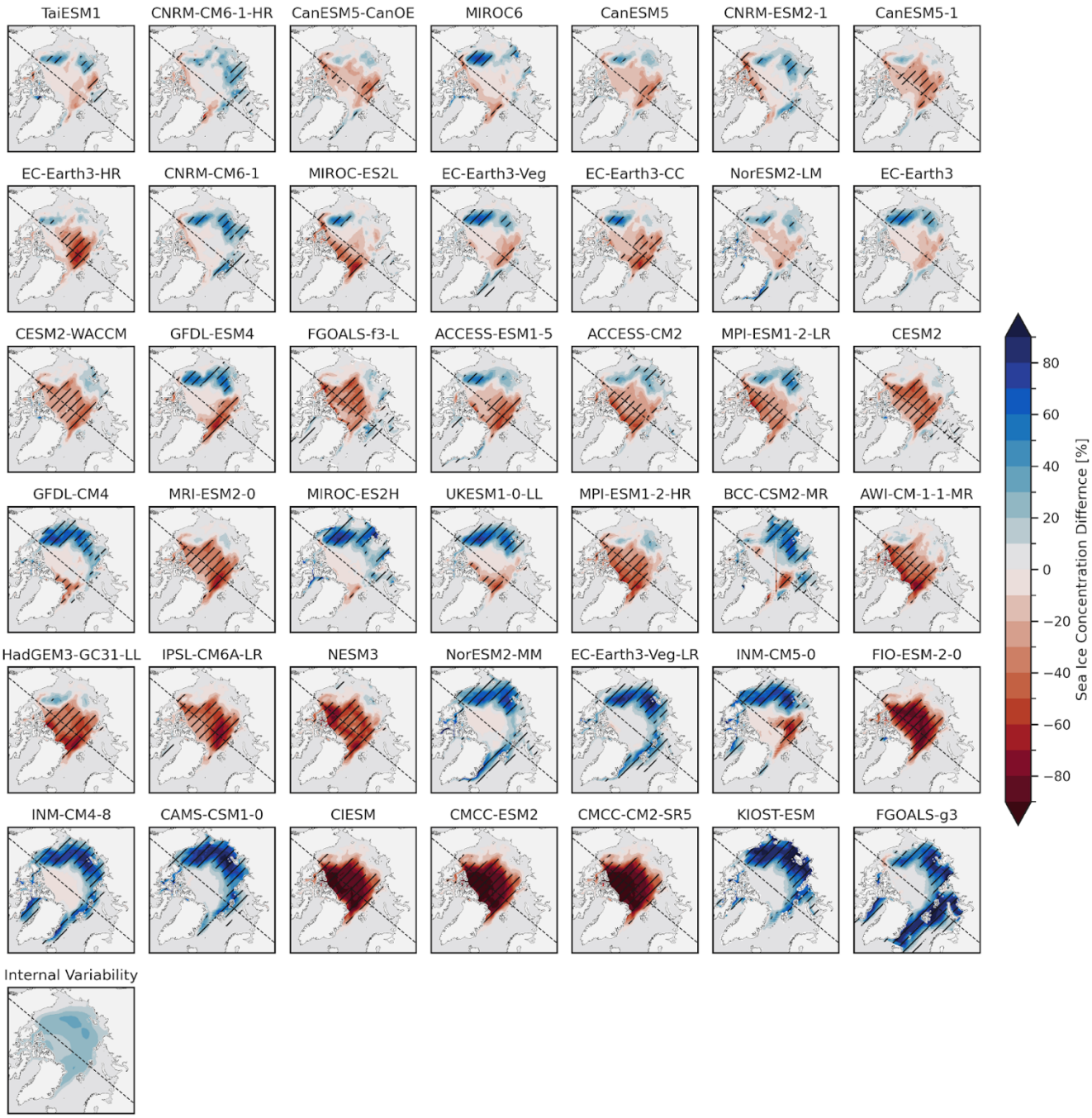

160 **Figure S28:** As in Fig. 11 of the main manuscript but for September sea ice concentration.

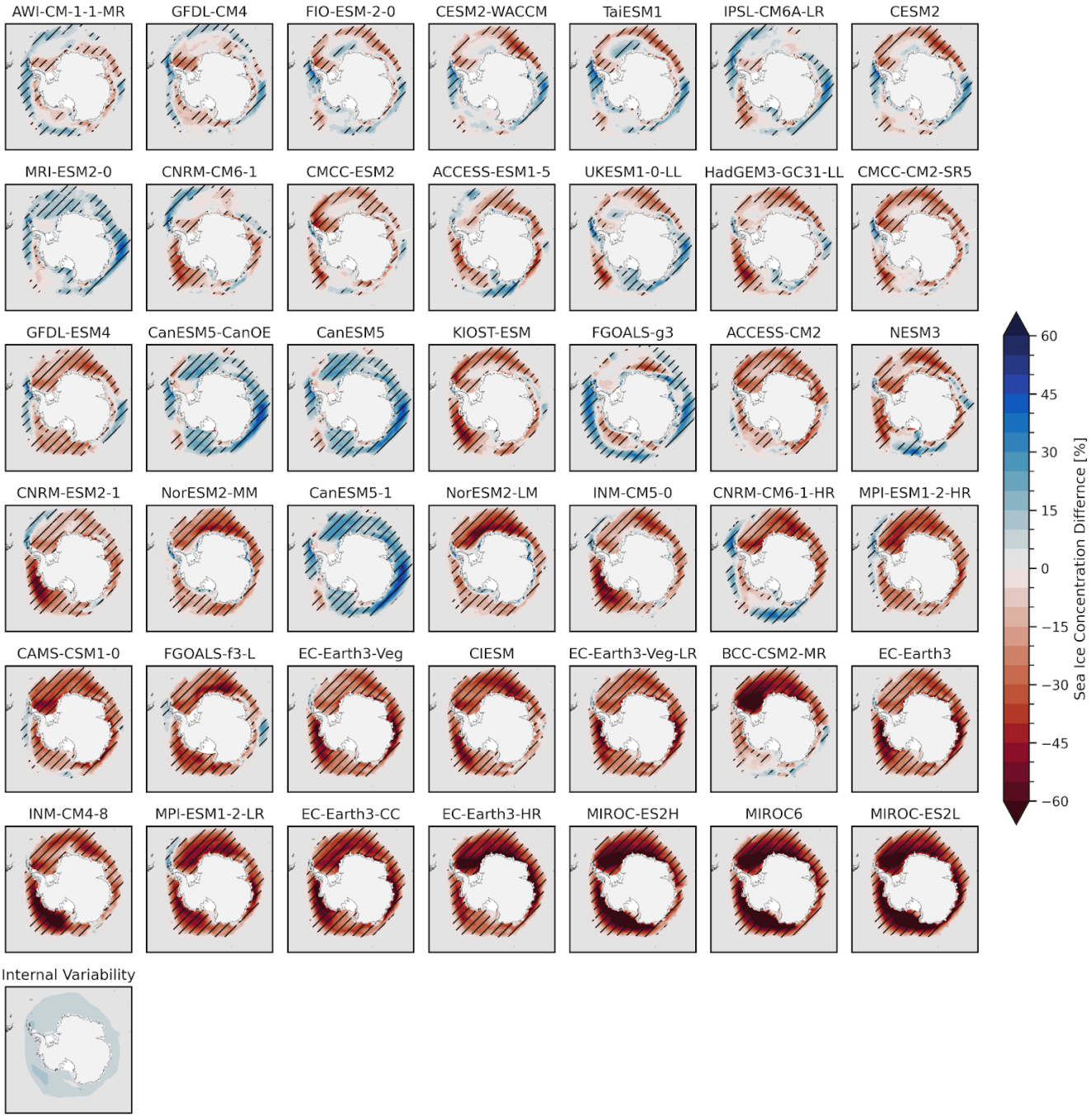

165 **Figure S29:** As in Fig. 13 of the main manuscript but for Annual sea ice area.

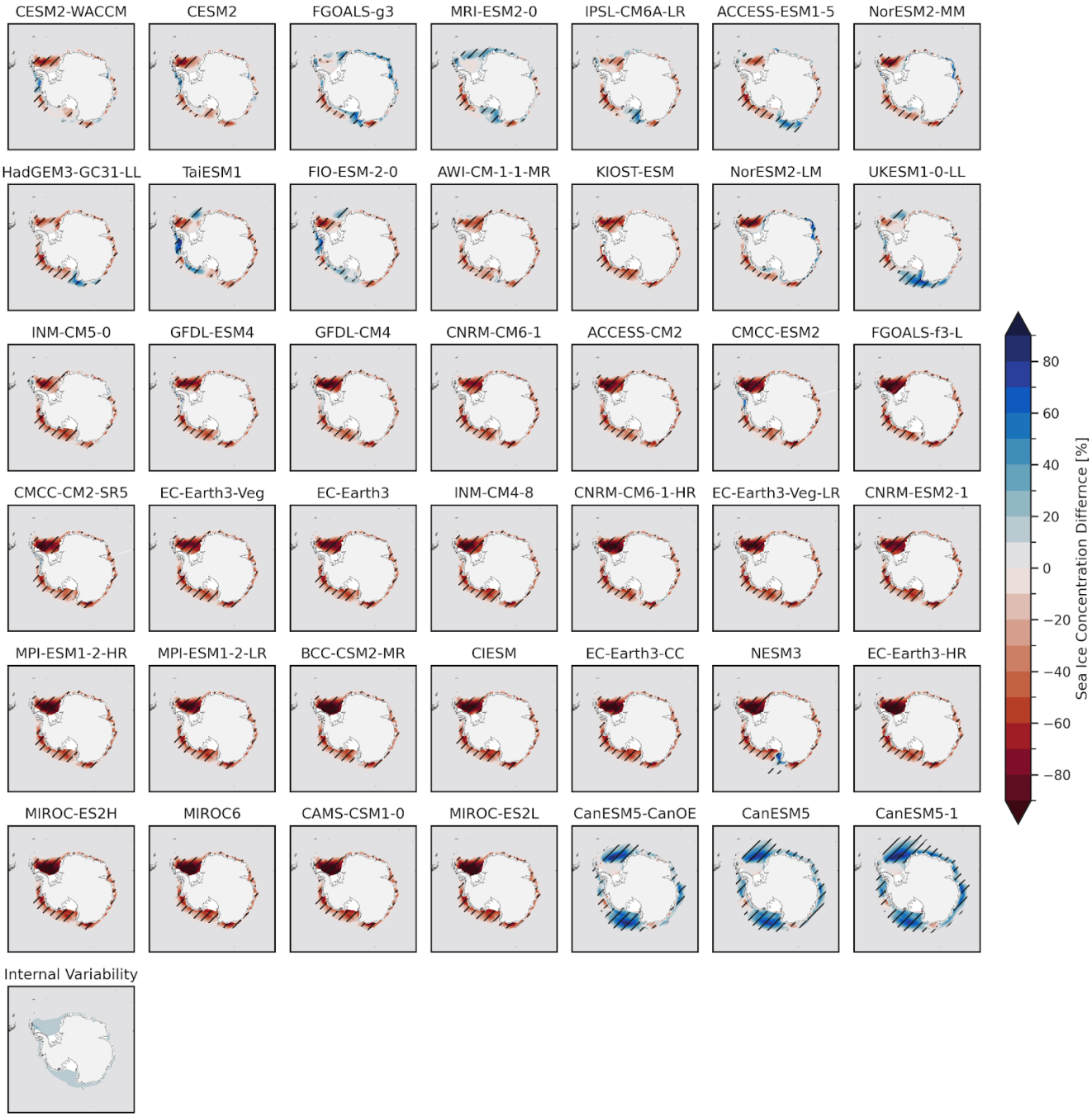

Figure S30: As in Fig. 13 of the main manuscript but for March sea ice area.

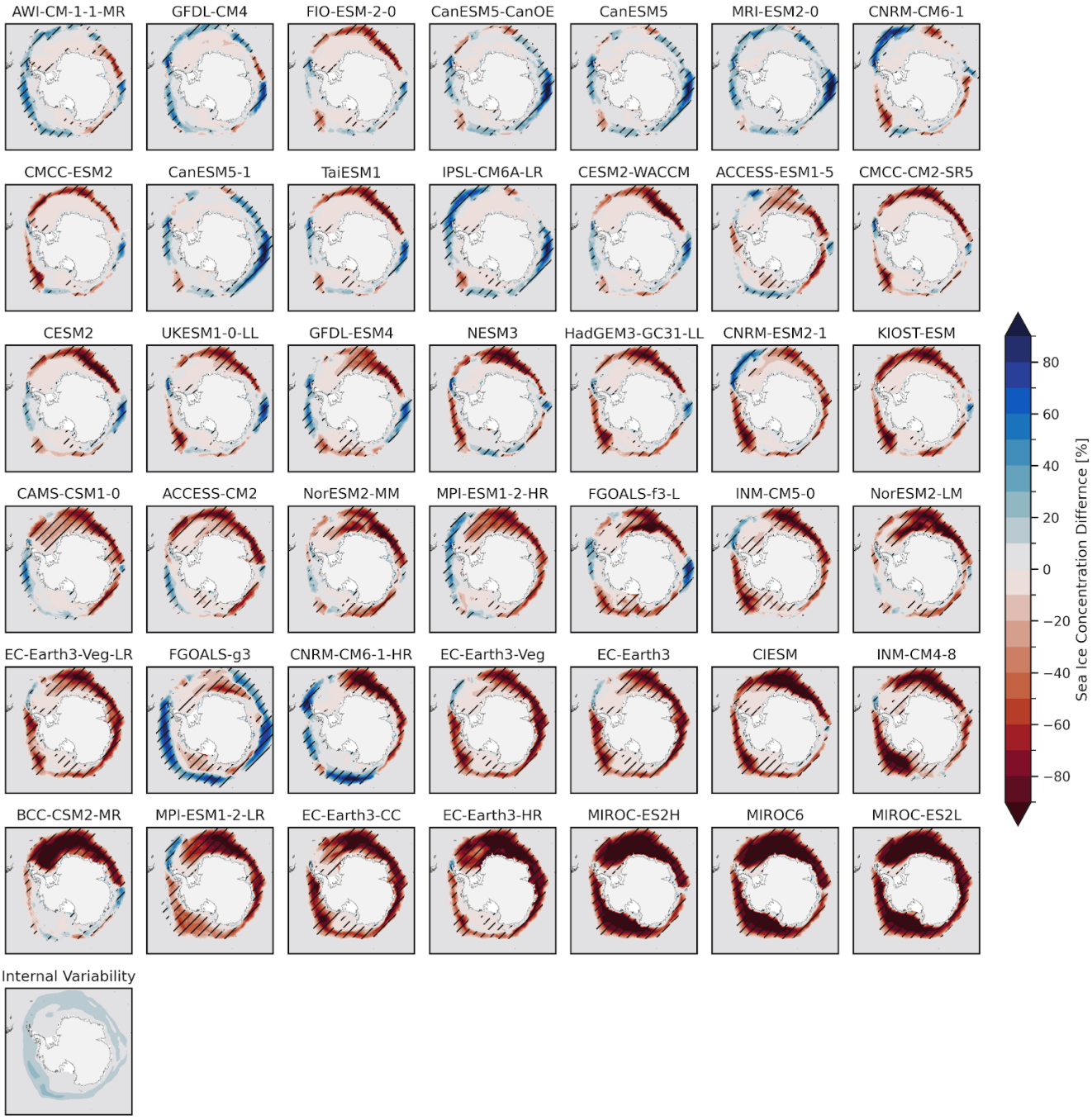

Figure S31: As in Fig. 13 of the main manuscript but for September sea ice area.

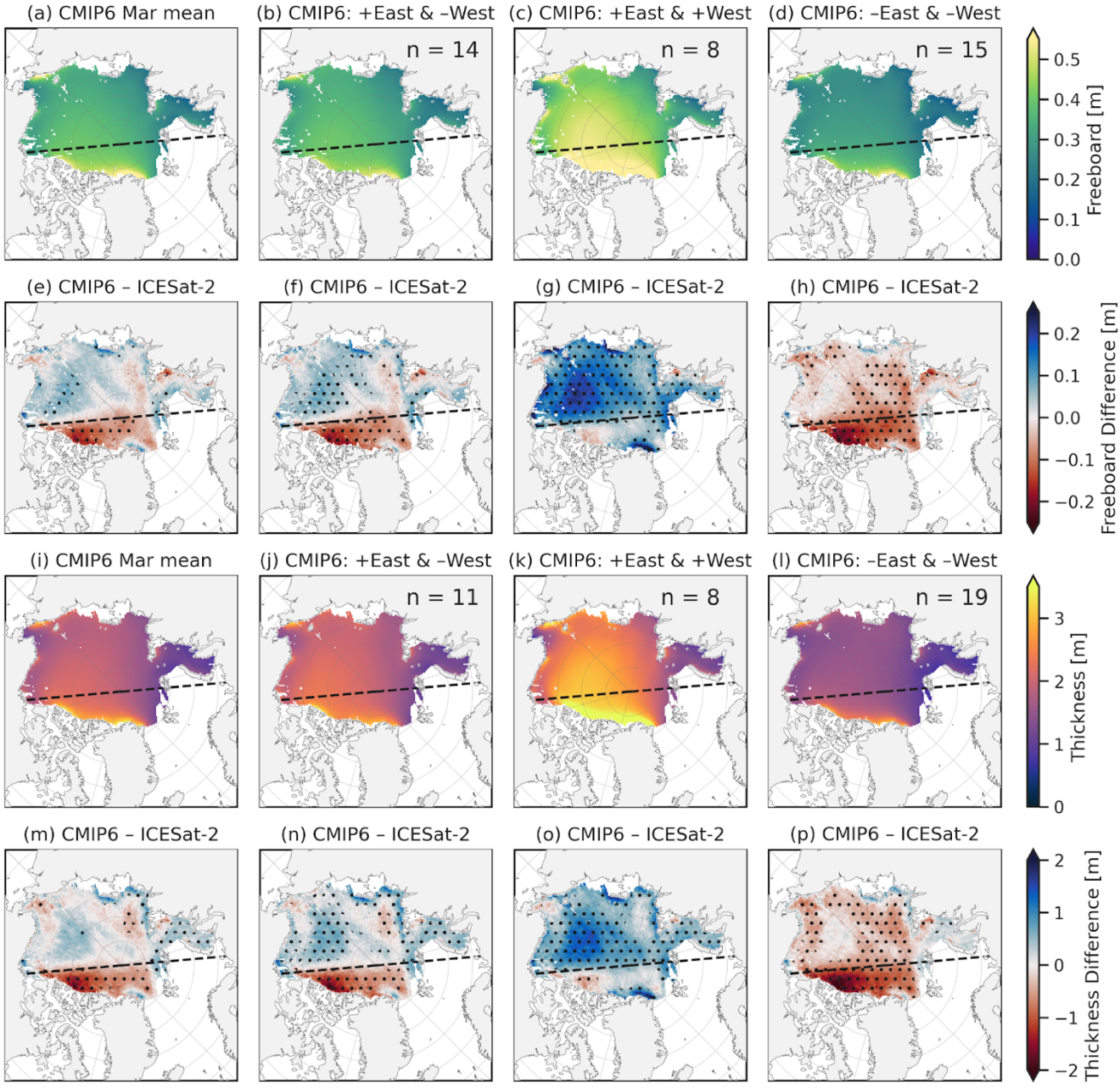

Figure S32: As in Fig. 12 of the main manuscript but for March.

185

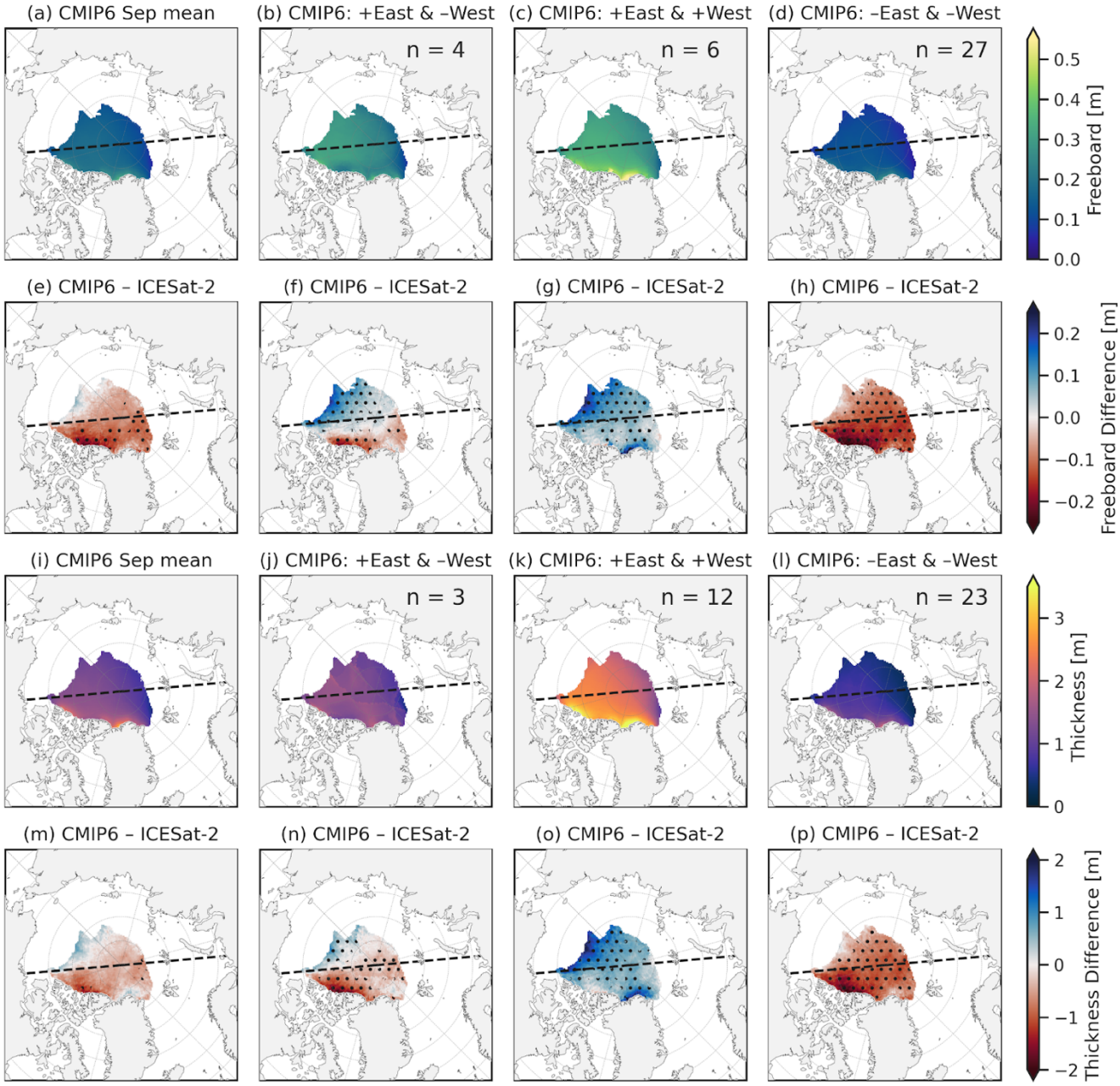

Figure S33: As in Fig. 12 of the main manuscript but for September.

190

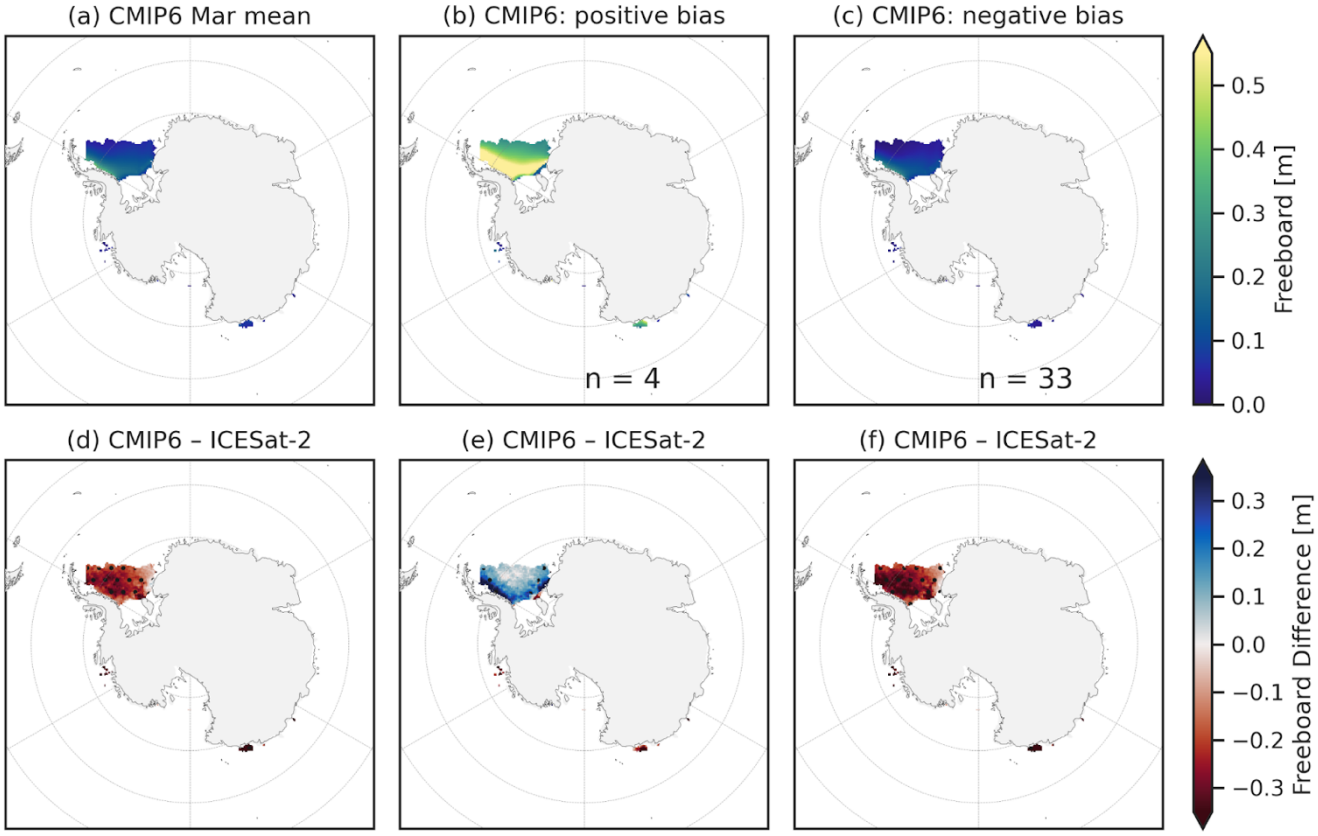

Figure S34: As in Fig. 14 of the main manuscript but for March.

195

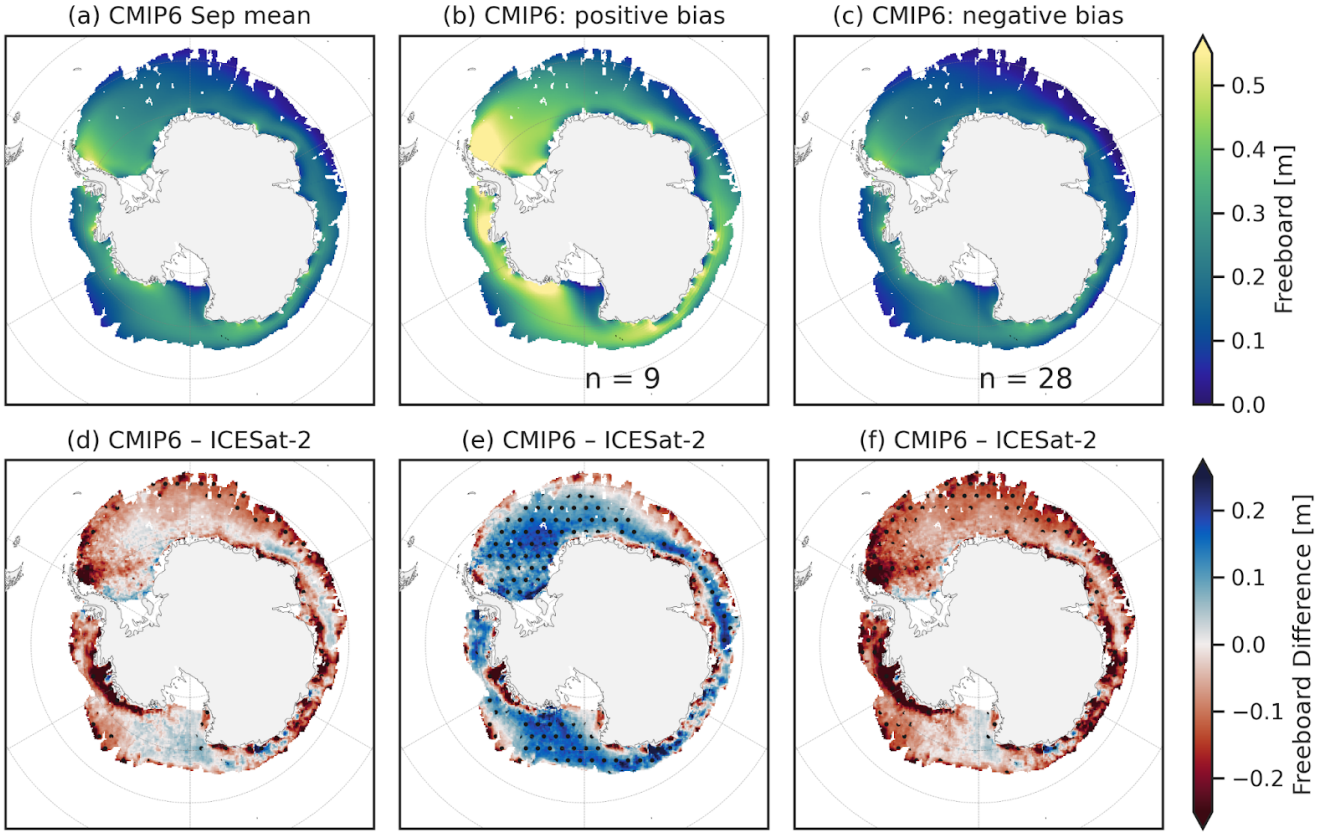

Figure S35: As in Fig. 14 of the main manuscript but for September.

200